EFFECT OF YAW-TILTED HINGE AXIS ON DEPLOYMENT ROBUSTNESS OF MARS AIRPLANE

Koji Fujita*, Hiroki Nagai, and Akira Oyama***

*** Institute of Space and Astronautical Science, Japan Aerospace Exploration Agency**
3-1-1, Yoshinodai, Chuo-ku, Sagamihara, Kanagawa, 252-5210, Japan
Tel.: +81-50-3362-4801 Fax.: +81-42-759-8260
fujita@flab.isas.jaxa.jp

**** Institute of Fluid Science, Tohoku University, Sendai, Miyagi, 980-8579, Japan**

Keywords: UAV, Low Reynolds number, Folding wing, Parametric study, Mars exploration

Abstract

This paper investigates the robustness of the aerial deployment behavior of the foldable-wing airplane for Mars exploration especially focused on the effect of the hinge axis tilting in a yaw direction. This study deals with four dispersive parameters for the robustness evaluation: drop velocity, surrounding gust velocity, initial pitch angle, and height. The robustness of several tilted and non-tilted hinge axis designs are calculated and then compared. The result clearly shows that the tilted hinge axis design can deploy with lower torque than the torque of the non-tilted hinge axis design. The increase of sideslip angle due to the hinge axis tilting suppressed an aerodynamic force on the deploying wing.

1 Introduction

A folding wing is an effective deployment mechanism for the airplane that is used for Mars exploration. A Mars airplane of Japan has been planned to perform aerial deployment using spring loaded hinges [1,2].

Figure 1 shows an aerial deployment process. Note that the vertical tail in this figure mounted on down side. At first, the right and left wings were folded under the fuselage. Then both wings rotated around the hinges. The rotation stopped when the wings aligned with the center. In this paper, the left wing always started deploying at the beginning of the simulation. On the other hand, the right wing did not start deploy at first. The right wing deployed after the deployment delay time T_{SR}.

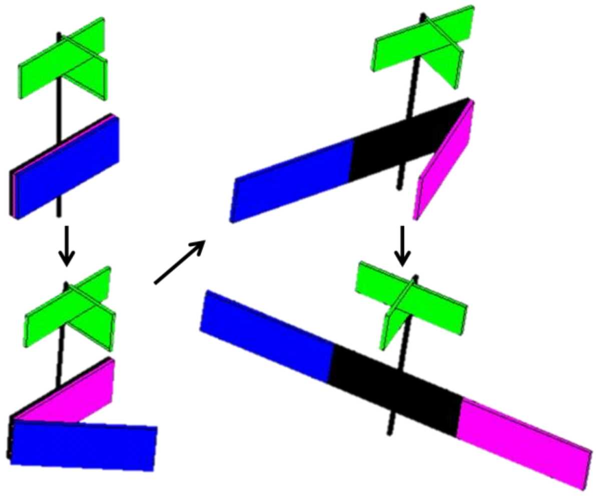

Fig. 1. Aerial Deployment Process.

A hinge torque is one of the primitive design variables to control the aerial deployment behavior. The required hinge torque is directly concerned with the deployment mechanism mass. In the past design, a large deployment torque was required and therefore the deployment mechanism was heavy [3]. Since the Mars airplane requires thorough mass reduction, it is necessary to reduce the required hinge torque while keeping high robustness of the aerial deployment. To reduce the required deployment mechanism torque, to fit the folded shape into the entry capsule, and to avoid a contact between right and left wings, this paper investigates the effect of the hinge axis tilting. Reference 4 studied the effect of the hinge axis tilting in a pitch direction and reported that the tilting can reduce required hinge torque by utilizing the aerodynamic assist for deployment through adjusting the angle of attack. The pitch-tilted hinge design was able to deploy without deployment mechanism torque at a certain condition. However the hinge axis tilting in a pitch direction has one problem that the hinge locates at out of the wing and therefore the hinge and its structural support protrude from the wing. This paper focused on the effect of the hinge axis tilting in a yaw direction. As shown in Fig. 2, the direction of the hinge axis was tilted at ν degrees within the XY plane of the body axis. Here, a positive direction of the hinge tilt angle was defined to be same to the rotation around the center body Z-axis.

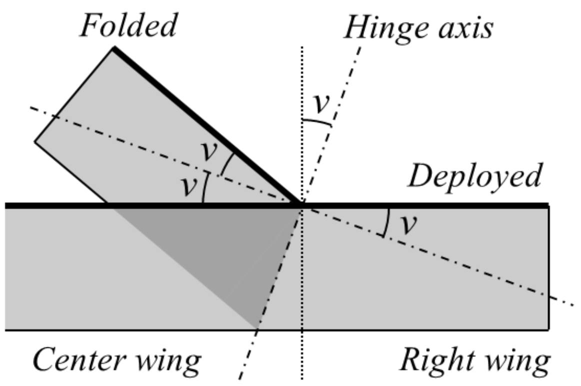

Fig. 2. Hinge Axis Tilting in a Yaw Direction. (Plan View)

2 Kinematic Analysis

To confirm a basic mechanism of the hinge axis tilting concept, a preliminary kinematic analysis was performed. Here, let us calculate the angle of attack and the sideslip angle of the outer wing under the fixed-center-body condition. This analysis method is based on Ref. 4.

2.1 Method

Rotation matrices were defined at first. Then an air velocity vector was defined and represented using the body coordinates of the outer wing. Finally the angle of attack and the sideslip angle of the outer wing were obtained using the components of the air velocity vector.

Rotation matrices for the rotations around X-axis $\mathbf{C}_X(\Theta)$, Y-axis $\mathbf{C}_Y(\Theta)$, and Z-axis $\mathbf{C}_Z(\Theta)$ can be written as follows:

$$\mathbf{C}_X(\Theta) \equiv \begin{bmatrix} 1 & 0 & 0 \\ 0 & \cos\Theta & \sin\Theta \\ 0 & -\sin\Theta & \cos\Theta \end{bmatrix}, \tag{1}$$

$$\mathbf{C}_Y(\Theta) \equiv \begin{bmatrix} \cos\Theta & 0 & -\sin\Theta \\ 0 & 1 & 0 \\ \sin\Theta & 0 & \cos\Theta \end{bmatrix}, \tag{2}$$

$$\mathbf{C}_Z(\Theta) \equiv \begin{bmatrix} \cos\Theta & \sin\Theta & 0 \\ -\sin\Theta & \cos\Theta & 0 \\ 0 & 0 & 1 \end{bmatrix}. \tag{3}$$

These matrices affect to rotate Θ degrees with respect to the specified axis.

Next, an air-velocity vector $\mathbf{V}_{O,air}$ was introduced in inertial system O. For simplicity, the flow was along the X-axis of the inertia system O.

$$\mathbf{V}_{O,air} = \begin{bmatrix} V_{air} \\ 0 \\ 0 \end{bmatrix}, \tag{4}$$

here the subscription O shows the coordinates of the vector representation.

From the definitions of the angle of attack and the sideslip angle, the body coordinates of the center body can be obtained by rotating the inertia coordinates O. First, the inertia coordinates O was rotated around Z_O axis. The rotation angle was same to the sideslip angle of the center body in the magnitude and opposite (i.e. left-handed screw) in the direction. After that the rotated coordinates was furthermore rotated around the Y-axis of the rotated coordinates. The rotation angle was same to the angle of attack of the center body in the magnitude and same (i.e. right-handed screw) in the direction. This coordinate transformation matrix can be written as

$$\mathbf{C}_{AO} = \mathbf{C}_Y(\alpha_A)\mathbf{C}_Z(-\beta_A). \tag{5}$$

Therefore the air velocity vector represented using the center body coordinates $\mathbf{V}_{A,air}$ is as follows:

$$\mathbf{V}_{A,air} = \mathbf{C}_{AO}\mathbf{V}_{O,air}. \tag{6}$$

The body coordinates of the outer wing can be obtained by rotating the body coordinates of the center body. First, the body coordinates of the center body was rotated around Z_A axis. The rotation angle was same to the tilt angle of the hinge in the magnitude and the direction. After that the rotated coordinates was furthermore rotated around the *X*-axis of the rotated coordinates. The rotation angle can be represented using the deployment angle θ_{dep}. Note that the directions of the rotation of the right and left wings were opposite. Finally the rotated coordinates was rotated again around the *Z*-axis of the rotated coordinates. The rotation angle was same to the tilt angle of the hinge in the magnitude and opposite in the direction. This coordinate transformation matrix can be written as follows:

for right wing

$$\mathbf{C}_{BA} = \mathbf{C}_Z(-\nu)\mathbf{C}_X(\pi-\theta_{dep})\mathbf{C}_Z(\nu), \tag{7}$$

for left wing

$$\mathbf{C}_{CA} = \mathbf{C}_Z(-\nu)\mathbf{C}_X(\theta_{dep}-\pi)\mathbf{C}_Z(\nu). \tag{8}$$

In this description, let us focus on the left wing. The coordinate transformation matrix from inertial coordinates *O* to the left wing coordinates *C* was given by

$$\begin{aligned}\mathbf{C}_{CO} &= \mathbf{C}_{CA}\mathbf{C}_{AO}\\ &= \mathbf{C}_Z(-\nu)\mathbf{C}_X(\theta_{dep}-\pi)\mathbf{C}_Z(\nu)\mathbf{C}_Y(\alpha_A)\mathbf{C}_Z(-\beta_A).\end{aligned} \tag{9}$$

Therefore the air velocity vector represented using the left wing coordinates $\mathbf{V}_{C,air}$ is as follows:

$$\mathbf{V}_{C,air} \equiv \begin{bmatrix} U_{C,air} \\ V_{C,air} \\ W_{C,air} \end{bmatrix} = \mathbf{C}_{CO}\mathbf{V}_{O,air}. \tag{10}$$

Finally, the angle of attack and the sideslip angle of the left wing can be obtained using the definition of those angles as

$$\begin{aligned}\alpha_C &\equiv \tan^{-1}\frac{W_{C,air}}{U_{C,air}}\\ &= \tan^{-1}\frac{\mathbf{C}_{CO}(3,1)}{\mathbf{C}_{CO}(1,1)},\end{aligned} \tag{11}$$

$$\begin{aligned}\beta_C &\equiv \sin^{-1}\frac{V_{C,air}}{\sqrt{U_{C,air}^2+V_{C,air}^2+W_{C,air}^2}}\\ &= \sin^{-1}\frac{\mathbf{C}_{CO}(2,1)}{\sqrt{\{\mathbf{C}_{CO}(1,1)\}^2+\{\mathbf{C}_{CO}(2,1)\}^2+\{\mathbf{C}_{CO}(3,1)\}^2}}.\end{aligned} \tag{12}$$

In the expression of the angle of attack and sideslip angle, we can rewrite these angles using only the entries of the coordinate transformation matrix $\mathbf{C}_{CO}$ because the air speed V_{air} assumed in Eq. (4) is canceled-out. Note that this analysis ignored an effect of motion. In the actual flight, the relative air velocity vector also changes due to the motions of the center body and outer wing.

The angle of attack and the sideslip angle of the left wing under the fixed-center-body condition were calculated. Here, the angle of attack and the sideslip angle of the center body were fixed to 10 degrees and 0 degree, respectively.

2.2 Results and Discussion

Figure 3 shows relations between the deployment angle and the angle of attack of the left wing. Three lines show the results of the tilt angle of -5, 0, and 5 degrees. The plot of the angle of attack of the left wing included negative value. When the angle of attack is negative, a lift force acts on folding direction since the wings were folded under the center body. The angle of attack increased as the tilt angle decreased. The positive angle of attack generates the lift force in deploying direction, which is expected to help deployment.

Figure 4 shows relations between the deployment angle and the sideslip angle of the left wing. At the folded condition, the sideslip angle was same to the double of the tilt angle, as shown in Fig. 1. The lift force decreases as the magnitude of the sideslip angle increases. Therefore, the hinge axis tilting in a yaw direction has an effect to suppress the influence of the aerodynamic force to the deployment.

As shown above, it seems that the hinge axis tilting concept is effective for helping deployment.

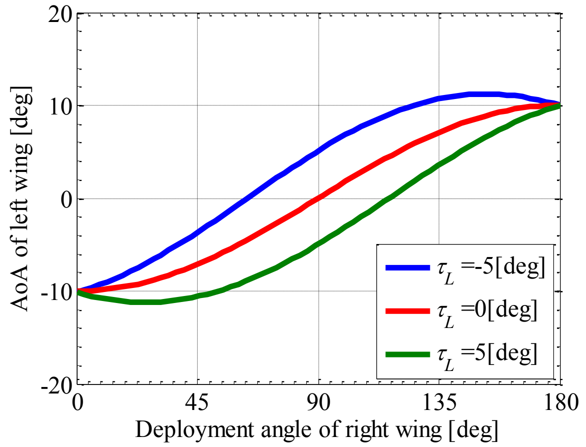

Fig. 3. Angle of Attack of Left Wing under Fixed-Center-Body Condition.

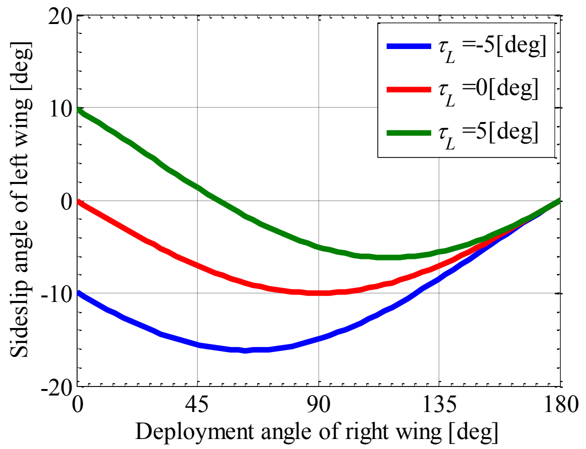

Fig. 4. Sideslip Angle of Left Wing under Fixed-Center-Body Condition.

3 Robustness Evaluation

Aerial deployment motions were simulated under the several dispersive conditions. The effect of the hinge axis tilting in a yaw direction on the robustness of the aerial deployment was evaluated.

3.1 Method

This evaluation used the aerial deployment motion simulator in Ref. 5. The analysis model consisted of three rigid bodies: a center, a right wing, and a left wing. The center consisted of a center wing, a fuselage, and a tail. The right and left wings were assumed as a flat plate. Each body was connected by hinges. The hinge axis of the non-tilted design is defined to be parallel to the *X*-axis of the center body coordinates. This study applied aerodynamic characteristics of a flat plate to the wings and the tail as basic characteristics. A drive power due to deployment mechanism was affected on the hinges as a torque. The deployment mechanism torque was obtained as a function of the deployment torque scale *F* in Ref. 5. The specifications of the rigid bodies were defined based on those of the Mars airplane [1]. The nominal initial condition was the dropping condition with aiming an airplane nose downward at a velocity of 65 m/s. The left wing started deployment when the simulation starts. The right wing started deployment after the right wing deployment delay time T_{SR}.

The conditions to judge whether the deployment succeeded or failed followed the definition in Ref. 5, as shown in Table 1. The margins of the airplane state for the conditions are set to the evaluation functions of the safety. The robustness was evaluated using the sigma level [6]. It is a function of the average and standard deviation of the evaluation functions. The sigma level *n* indicates the probability that the evaluation function violates the constraints. The sigma level *n* was defined as follows:

$$n \equiv \min\left(\frac{\mu_f - LSL}{\sigma_f}, \frac{USL - \mu_f}{\sigma_f}\right), \tag{13}$$

where *LSL* and *USL* are the Lower / Upper Specification Limits. μ_f and σ_f are the average and the standard deviation of the evaluation function *f*. The average and the standard deviation were calculated using sensitivity method. The sensitivity was numerically obtained using a few simulations. In this paper, a total minimum sigma level was defined as a minimum value of the sigma level of all evaluation functions and all dispersive input variables for each design point.

The design variables for each robustness analysis were the deployment torque scale *F* and the right wing deployment delay time T_{SR}. They are the variables directly concerning the aerial deployment. The ranges of those were set from 0 to 1.5 and from 0 to 2 seconds, respectively.

Five types of the hinge tilt angle settings were studied. The tilt angles of the right and left hinges υ_R, υ_L were set to -5, 0, and 5 degrees. Note that a positive direction was set to right-hand screw direction of the center body *Z*-axis.

A scope of the disturbance was defined in Ref. 5. considering the aerial deployment condition on Mars. The dispersive input variables were drop velocity, surrounding gust velocity, initial pitch angle, and height.

Finally representative conditions were selected and then its deployment behaviors were compared.

Table 1. Safe Deployment Judgment Condition [5].

Name	*Limitation* *Low*	~	*High*	*Unit*
Load factor	-1	~	5	-
Hinge reaction moment	-	~	12	N·m
Main wing bending moment	-5	~	26	N·m

3.2 Results and Discussion

Figure 5 shows the total minimum sigma level of the non-tilted design. The legend "Success" means both wings were fully deployed and all safe deployment judgment conditions were satisfied. The legend "Danger" means both wings were fully deployed however at least one of the safe deployment judgment conditions was violated. The legend "Failure" means the right or left wing was not fully deployed or the right wing tip hit the left wing. The lower limit of the successful deployment torque scale was 0.26.

Figure 6 shows the total minimum sigma level of the right and left hinge tilt angle of 5 degrees design. The lower limit of the successful deployment torque scale was 0.38, which was higher than the non-tilted design.

Figure 7 shows the total minimum sigma level of the design of the right and left hinge tilt angle of 5 and -5 degrees, respectively. The lower limit of the successful deployment torque scale was 0.23, which was slightly lower than the non-tilted design. The successful design range was enlarged.

Figure 8 shows the total minimum sigma level of the design of the right and left hinge tilt angle of -5 and 5 degrees, respectively. The lower limit of the successful deployment torque scale was 0.34, which was higher than the non-tilted design.

Figure 9 shows the total minimum sigma level of the right and left hinge tilt angle of -5 degrees design. The lower limit of the successful deployment torque scale was 0.19, which was lower than the non-tilted design. The successful design range was enlarged.

Figure 5-9 indicate that the lower limit of the successful deployment torque scale expanded to low torque region as the right and left hinge tilt angle decreased. However, all simulated hinge axis tilting condition required some deployment mechanism torque, although the hinge axis tilting in a pitch direction does not required the deployment mechanism torque [4]. Therefore the effect of the hinge axis tilting in a yaw direction was smaller than the effect of the tilting in a pitch direction.

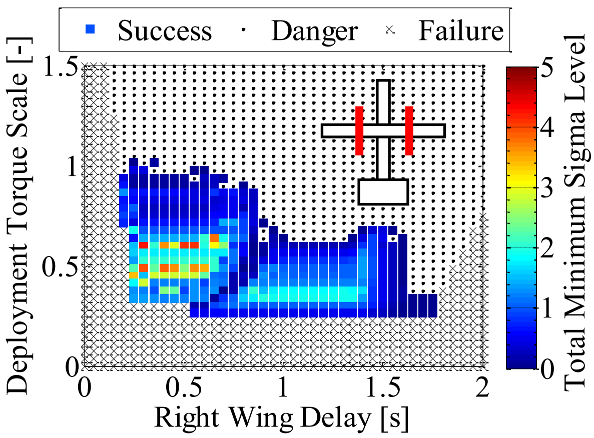

Fig. 5. Total Minimum Sigma Level with Non-Tilted Condition.

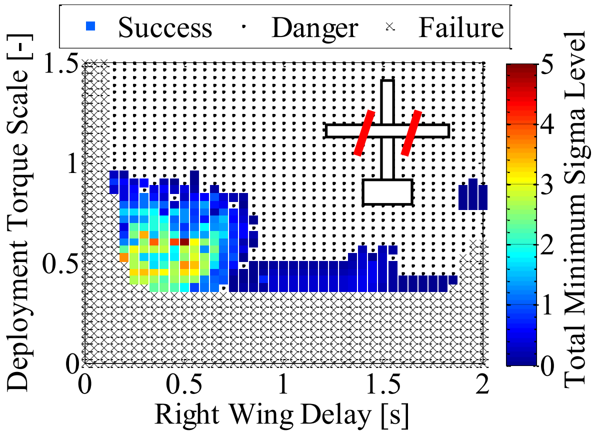

Fig. 6. Total Minimum Sigma Level with Right and Left Hinge Tilt Angle of 5 Degrees and 5 Degrees Condition.

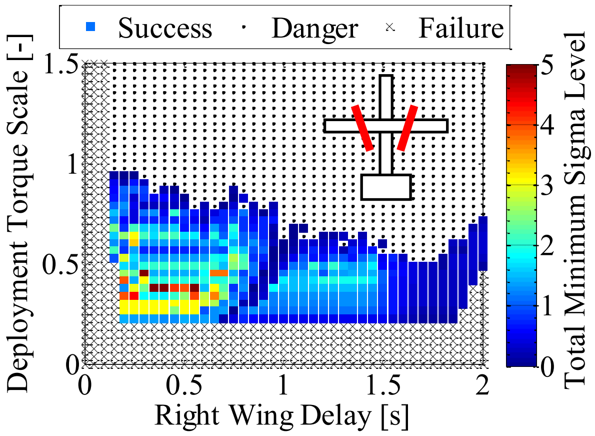

Fig. 7. Total Minimum Sigma Level with Right and Left Hinge Tilt Angle of 5 Degrees and -5 Degrees Condition.

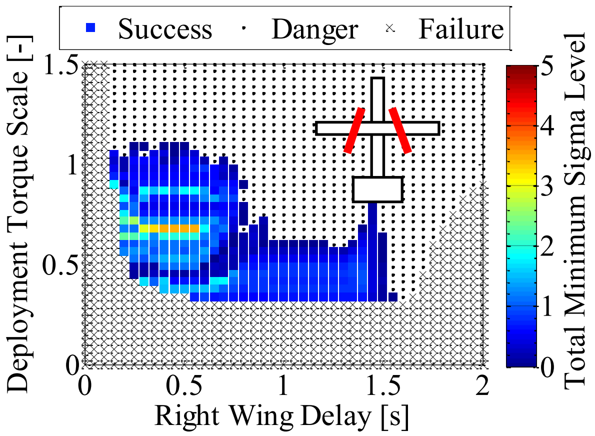

Fig. 8. Total Minimum Sigma Level with Right and Left Hinge Tilt Angle of -5 Degrees and 5 Degrees Condition.

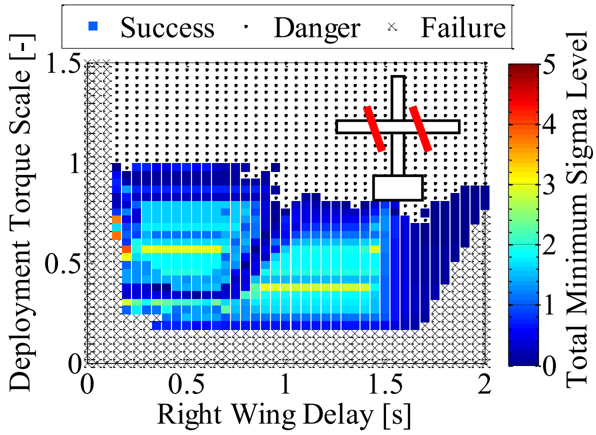

Fig. 9. Total Minimum Sigma Level with Right and Left Hinge Tilt Angle of -5 Degrees and -5 Degrees Condition.

As a representative condition, the deployment torque scale F and the right wing deployment delay time T_{SR} were selected to 0.3 and 0.3 seconds, respectively. As shown in Figs. 5 and 7, the airplane failed aerial deployment with non-tilted design and succeeded with tilted design.

Figures 10 and 11 show the time histories of the angle of attack and the sideslip angle of each body with non-tilted condition. At the beginning, the angle of attack of the right and left wings were negative. Therefore lift force acted to folding direction. This force overcame the deployment mechanism torque and prevented from deploying.

On the other hand, Figs. 12 and 13 show the time histories of the angle of attack and the sideslip angle of each body with the right and left hinge tilt angle of 5 degrees and -5 degrees. Initial angle of attack was negative like the non-tilted condition. However, the magnitude of the sideslip angle of the left wing was higher than the non-tilted condition due to the hinge axis tilting. Therefore the lift force was reduced and the left wing succeeded deployment in low deployment torque scale condition. For the same reason the robustness also improved by hinge axis tilting, as shown in Fig. 7.

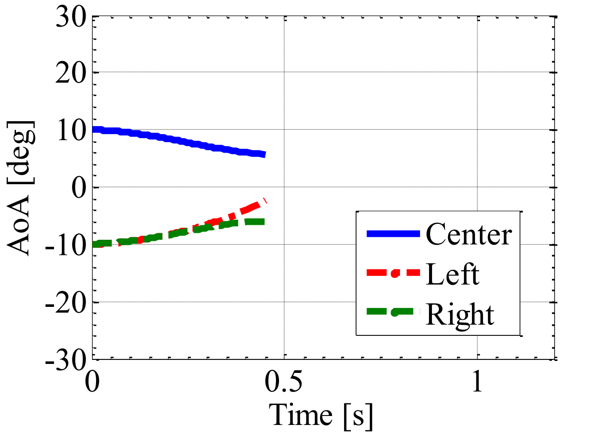

Fig. 10. Time history of Angle of Attack with Non-Tilted Condition.

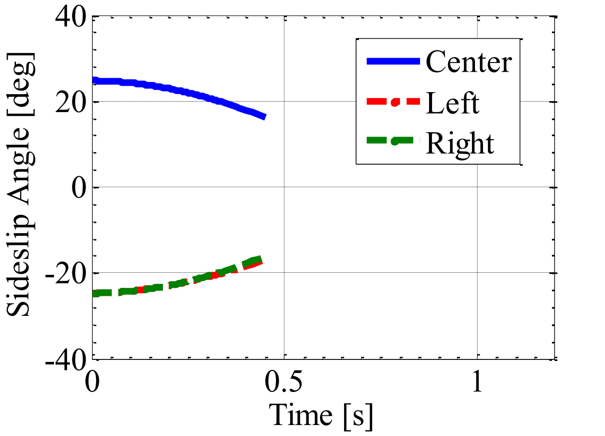

Fig. 11. Time history of Sideslip Angle of with Non-Tilted Condition.

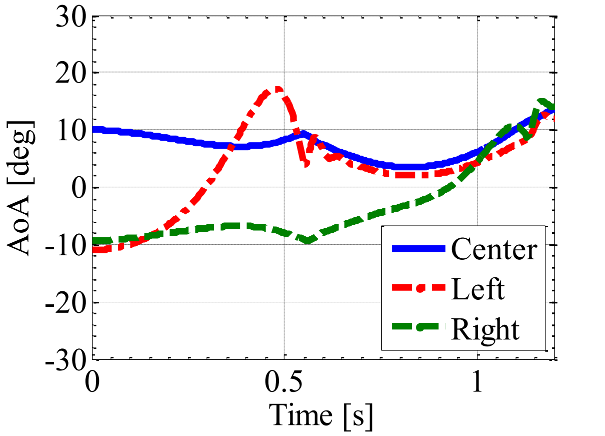

Fig. 12. Time history of Angle of Attack with Right and Left Hinge Tilt Angle of 5 Degrees and -5 Degrees Condition.

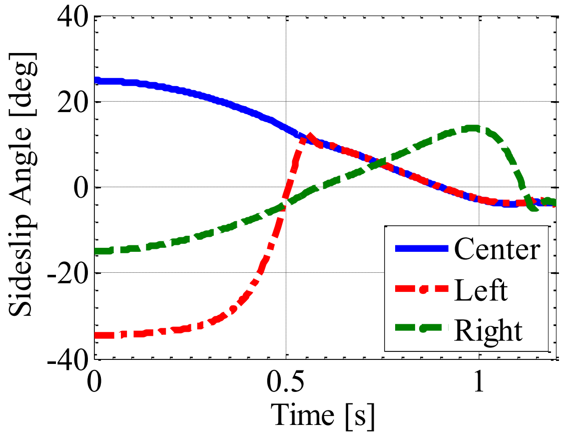

Fig. 13. Time history of Sideslip Angle of with Right and Left Hinge Tilt Angle of 5 Degrees and -5 Degrees Condition.

4 Conclusion

The kinematic analysis of the hinge axis tilting in a yaw direction revealed that the hinge axis tilting in a yaw direction has an effect to suppress the influence of the aerodynamic force to the deployment by increasing the sideslip angle. The Simulations of the aerial deployment motion of the Mars airplane with and without hinge axis tilting were performed. The hinge axis tilting in a yaw direction lowered the required deployment torque, enlarged the successful design range, and increased robustness. Utilizing the effect of the hinge axis tilting allows the deployment actuator to reduce its torque. Therefore the airplane could achieve saving weight. Note that the increase of the sideslip angle can reduce the absolute value of the lift force on the outer wing, however cannot change the direction of the lift force. Therefore the yaw-tilted hinge design requires some deployment actuators although the pitch tilted hinge design does not require it. In that sense, the effect of the hinge axis tilting in a yaw direction was smaller than the effect of the tilting in a pitch direction.

References

[1] Nagai H, Oyama A, Mars Airplane WG. Development of Mars Exploration Aerial Vehicle in Japan. *Proceedings of the 30th International Symposium on Space Technology and Science*, 2015-k-46, Kobe, Japan, July, 2015.

[2] Fujita K, Motoda T, Nagai H. Numerical Analysis for an Aerial Deployment Motion of a Folded-Wing Airplane. *Proceedings of the AIAA SciTech2014*, AIAA 2014-0383, National Harbor, Maryland, USA, January, 2014.
[3] Fujita, K. A Parametric Study of the Deployable Wing Airplane for Mars Exploration. *Proceedings of the 29th Congress of the International Council of the Aeronautical Sciences*, St. Petersburg, Russia, 1.10 UAS1, 2014-0478, Sep., 2014.
[4] Fujita K, Nagai N, Oyama A. Robust Aerial Deployment of Mars Airplane with Tilted Folding-Axis. *Proceedings of the AIAA SciTech2016*, AIAA 2016-0023, San Diego, California, USA, January, 2016.
[5] Fujita K, Nagai N. Robustness Analysis on Aerial Deployment Motion of a Mars Airplane using Multibody Dynamics Simulation: Effects of Wing-Unfolding Torque and Timing. *Proceedings of the 7th Asia-Pacific International Symposium on Aerospace Technology*, Cairns, Australia, November, 2015.
[6] Shimoyama K, Oyama A, Fujii K. A New Efficient and Useful Robust Optimization Approach - Design for Multi-Objective Six Sigma. *Proceedings of the 2005 IEEE Congress on Evolutionary Computation*, Vol. 1, 2005, pp. 950–957.

Copyright Statement